

OXYGEN ISOTOPIC VARIATIONS IN A FLUFFY TYPE A CAI FROM THE VIGARANO METEORITE.

K. Harazono¹ and H. Yurimoto¹, ¹Department of Earth and Planetary Sciences, Tokyo Institute of Technology, 2-12-1 Ookayama, Meguro, Tokyo 152-8551, Japan (kharazon@geo.titech.ac.jp).

Introduction: Coarse-grained Ca-Al-rich inclusions (CAIs) are classified into Type A, B and C [1]. Type B and compact Type A CAIs are believed that they were formed from molten drops [2, 3]. On the other hand, fluffy Type A CAIs are believed that they were formed by gas-solid condensation, because of their extremely irregular shapes and reversely-zoned melilite crystals [4]. Recent ion microprobe analyses show that ¹⁶O-rich and ¹⁶O-poor melilite coexist in a Type B or compact Type A CAI directly indicating oxygen isotopic exchange during the formation [e.g. 5]. However, such observation has not been made in fluffy Type A CAIs.

Distributions of oxygen isotopes in Type A CAIs have been characterized as: spinel, hibonite and pyroxene are ¹⁶O-rich ($\delta^{17,18}\text{O} \sim -40\text{‰}$) while melilite is usually ¹⁶O-poor ($\delta^{17,18}\text{O} \sim 0\text{‰}$) [6, 7].

Here we report coexistence of ¹⁶O-rich and ¹⁶O-poor melilite in a fluffy Type A CAI from the Vigarano meteorite. The discovery indicates that multiple heating processes in the solar nebula are required to form fluffy Type A CAIs.

Analytical Techniques: A coarse-grained CAI (V2-01) for a thin section of the Vigarano CV3 meteorite was studied by petrographic microscope and a scanning electron microscope (JEOL JSM-5310LV) equipped with energy dispersive X-ray spectrometer (Oxford LINK ISIS).

Oxygen isotopes were measured *insitu* by secondary ion mass spectrometry using multi-collection mode of the TiTech CAMECA IMS-1270. A Cs⁺ primary beam (20 keV, 0.6-2 nA) of 15-20 μm diameter was used. Both ¹⁶O⁻ and ¹⁸O⁻ were measured using off-axis Faraday cups at mass resolving power (MRP) ~ 2000 , while ¹⁷O⁻ was measured on the axial electron multiplier at MRP ~ 4500 , sufficient to separate interfering ¹⁶OH⁻. Measurements of background noises of Faraday cups were made and signals of ¹⁶O⁻ and ¹⁸O⁻ were corrected. In order to correct instrumental mass fractionation and matrix effect among minerals, five terrestrial minerals were used as standards for each mineral species: a synthetic gehlenite and $\ddot{\text{a}}$ kermanite, a Russian spinel, a Miyake-Jima anorthite and a Takashima augite. Internal precision (1σ) on $\delta^{17}\text{O}$ and $\delta^{18}\text{O}$ for each spot was typically $\sim 0.4\text{‰}$ and $\sim 0.4\text{‰}$, respectively. The reproducibility of terrestrial standards (1σ) on $\delta^{17}\text{O}$ and $\delta^{18}\text{O}$ was $\sim 0.7\text{‰}$ and $\sim 0.6\text{‰}$, respectively. Therefore precision of analyses (1σ) on $\delta^{17}\text{O}$ and $\delta^{18}\text{O}$ relative to SMOW was estimated $\sim 0.9\text{‰}$ and $\sim 0.8\text{‰}$, respectively, by

error propagation. We selected six melilite grains in the CAI and repeatedly measured them through this study to check any analytical drifts. The reproducibility of the analyses (1σ) on $\delta^{17}\text{O}$ and $\delta^{18}\text{O}$ was $\sim 0.9\text{‰}$ and $\sim 0.8\text{‰}$, respectively, consistent to the error estimation.

Results: A coarse-grained CAI (V2-01) is a fluffy shaped, fragmented inclusion of ~ 5 mm across. Wark-Lovering rim is present along the original edges of the inclusion. Rim has numerous embayments and large embayments sometimes exist, which are filled with accretionary rim. This CAI is dominated by coarse-grained melilite ($\geq 50 \mu\text{m}$). In addition, narrow range of $\ddot{\text{a}}$ kermanite compositions in melilite grains ($\ddot{\text{A}}\text{k}_{0-28}$) is similar to that in fluffy Type A CAIs [4]. These characteristics suggest that this CAI was a fluffy Type A CAI. As unique petrographic characteristic in this inclusion, layers of anorthite ($\sim 20 \mu\text{m}$) and pyroxene ($\sim 20 \mu\text{m}$) surround melilite like Wark-Lovering rim in the interior of this inclusion.

Although most melilite grains are spinel-free, some melilite grains poikilitically enclose spinel grains. Most spinel grains concentrate in the interior of the inclusion.

Fig.1 shows oxygen isotopic compositions of individual minerals in V2-01. All phases except melilite are ¹⁶O-rich ($\delta^{18}\text{O} \sim -45\text{‰}$ and $\sim -33\text{‰}$ for anorthite), while melilite has wide range of oxygen isotopes from ¹⁶O-rich to ¹⁶O-poor ($\delta^{18}\text{O}$ ranges between -48‰ and 13‰). Although ¹⁶O-poor melilite is dominant in the inclusion, each melilite grain sometimes has different oxygen isotopic compositions and directly contacts each other.

In this CAI, oxygen isotopic compositions in melilite vary with $\ddot{\text{a}}$ kermanite compositions. $\ddot{\text{A}}$ k-poor melilite ($\leq \ddot{\text{A}}\text{k}_6$) is ¹⁶O-rich ($\delta^{18}\text{O}$ ranges between -48‰ and -40‰). $\ddot{\text{A}}$ k-rich melilite ($\geq \ddot{\text{A}}\text{k}_{17}$) is ¹⁶O-poor ($\delta^{18}\text{O}$ range between -2‰ and 13‰). Melilite with intermediate $\ddot{\text{a}}$ kermanite compositions ($\ddot{\text{A}}\text{k}_{6-17}$) gives wide range of oxygen isotopic compositions ($\delta^{18}\text{O}$ ranges between -35‰ and 13‰). Some melilite grains are contact with each other with almost homogenous $\ddot{\text{a}}$ kermanite compositions ($\ddot{\text{A}}\text{k}_{8-10}$), while their oxygen isotopic compositions differ by crystals (Fig.2). $\ddot{\text{A}}$ k-poor, ¹⁶O-rich melilite grains are found only near Wark-Lovering rim.

Some melilite grains have small oxygen isotopic zoning in a single crystal. The range of isotopic zoning is 5-10‰. This isotopic zoning is almost parallel to CCAM line.

Discussion: Grains of ¹⁶O-poor melilite are from $\sim 50 \mu\text{m}$ blocky grains to laths shape (500 μm long and

200 μm wide). Since these grain sizes are much coarser than those in fine-grained CAIs, aqueous alteration process is implausible to the origin of oxygen isotopic depletion of melilite in this CAI [8].

Melilite condenses prior to spinel from solar nebula gas [9]. On the other hand, spinel crystallizes prior to melilite from liquid of Type A composition [10]. The poikilitic texture of melilite and spinel indicates that melilite crystallized from liquid. The liquid would be formed by direct condensation from solar nebula [11] or melting of CAI precursors. In either case, fluffy shape of this CAI indicates that small liquid/solid ratio was maintained during the formation. Spinel-bearing melilite has wide range of oxygen isotopic compositions ($\delta^{18}\text{O}$ ranges between -30‰ and 11‰). The heterogeneous oxygen isotopic compositions suggest change of oxygen isotopic compositions of gaseous reservoir or incomplete isotopic exchange between melt and gaseous reservoir.

Because melilite grains in Fig. 2 have homogenous $\delta^{18}\text{O}$ compositions, these grains would have crystallized at the same temperature. If these melilite formed by liquid condensation processes, oxygen isotopic variations of these grains suggest that liquid condensed repeatedly from gaseous reservoir with different oxygen isotopic composition. The CAI became large through the multiple condensations. If these melilite formed by incomplete melting processes, the CAI would be originally ^{16}O -rich, because degree of ^{16}O -enrichment of melilite correlated to the gehlenite content. Gehlenitic melilite is difficult to remelt through reheating process. Therefore oxygen isotopic variations suggest that partial melting of $\delta^{18}\text{O}$ -rich melilite occurred repeatedly and oxygen isotopic exchange occurred between ^{16}O -rich melt and ^{16}O -poor gas. In either case, this CAI would have been formed through multiple heating processes in the solar nebula.

Isotopic drifts from CCAM line can be seen both in ^{16}O -rich and ^{16}O -poor components. The drift is observed in whole crystal for some melilite grains and also observed in part of a crystal for some melilite grains. These drifts would be caused by secondary process like aqueous alteration after the oxygen isotopic exchange along CCAM line.

References: [1] MacPherson et al. (1988) in *Meteorites and the Early Solar System*, 746. [2] MacPherson G. J. and Grossman L. (1981) *EPSL*, 52, 16. [3] Simon S. B. et al. (1999) *GCA*, 63, 1233. [4] MacPherson G. J. and Grossman L. (1984) *GCA*, 48, 29. [5] Yurimoto H. et al. (1998) *Science*, 282, 1874. [6] Clayton R. N. et al. (1977) *EPSL*, 34, 209. [7] Clayton R. N. (1993) *Annu. Rev. Earth Planet. Sci.* 21, 115. [8] Fagan T. J. et al. (2002) *MAPS*, 37, A45. [9] Grossman L. (1972) *GCA*,

36, 597. [10] Stolper E. M. (1982) *GCA*, 46, 2159. [11] Yoneda S. and Grossman L. (1995) *GCA*, 59, 3413.

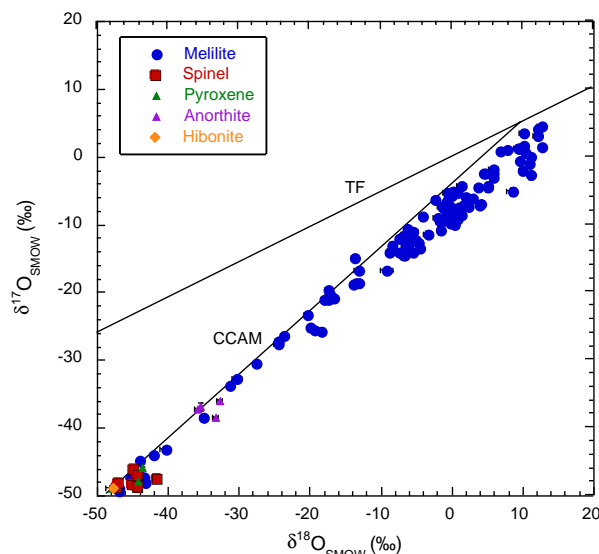


Fig. 1 Oxygen isotopic compositions of individual minerals in a coarse-grained CAI from the Vigarano meteorite.

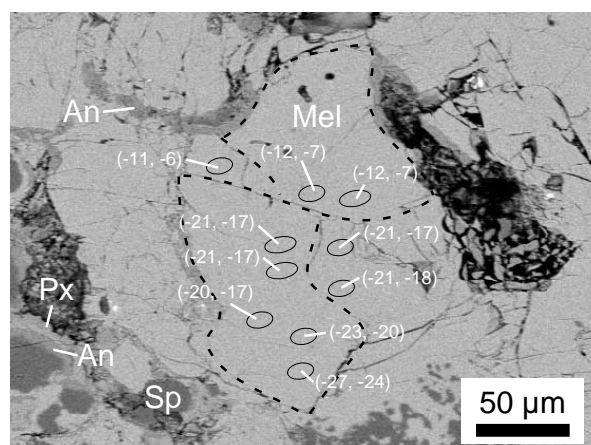


Fig. 2 Backscattered electron image of V2-01. Dashed lines show the grain boundary. Each open circle shows location of SIMS analysis with crater size and oxygen isotopic composition ($\delta^{17}\text{O}$, $\delta^{18}\text{O}$). Mel, melilite; Sp, spinel; An, anorthite; Px, pyroxene. Although melilite grains are homogenous with $\delta^{18}\text{O}$, their oxygen isotopic compositions differ by crystals. One melilite grain has isotopic zoning.